Proceedings of Eurotherm78 - Computational Thermal Radiation in Participating Media II
5-7 April 2006, Poitiers, France

Maximum Time-Resolved Hemispherical Reflectance of Absorbing and Isotropically Scattering Media

by Kyle Smith$^{(*)}$, Kamal Katika$^{(*)}$, and Laurent Pilon$^{(*)}$

(*) Mechanical and Aerospace Engineering Department
Henri Samueli School of Engineering and Applied Science
University of California, Los Angeles - Los Angeles, CA 90095, USA
Phone: +1 (310) 206-5598, E-mail: pilon@seas.ucla.edu

Abstract

This paper presents a parametric study of the time-resolved hemispherical reflectance of a plane-parallel slab of homogeneous, cold, absorbing, and isotropically scattering medium exposed to a collimated Gaussian pulse. The front surface of the slab is transparent while the back surface is assumed to be cold and black. The one-dimensional transient radiation transfer equation is solved using the modified method of characteristics. The parameters explored include (1) the optical thickness, (2) the single scattering albedo of the medium, and (3) the incident pulse width. The study pays particular attention to the maximum transient hemispherical reflectance and identifies optically thin and thick regimes. It shows that the hemispherical reflectance is independent of the optical thickness in the optically thick regime. In the optically thin regime, however, it depends on all three parameters explored. The transition between the optically thick and thin regimes occurs when the optical thickness is approximately equal to the dimensionless pulse width. Finally, correlations relating the maximum of the hemispherical reflectance as a function of the optical thickness, the single scattering albedo of the materials and the incident pulse width have been developed. These correlations could be used to retrieve radiation characteristics or serve as initial guesses for more complex inversion schemes accounting for anisotropic scattering.

Nomenclature

I Intensity
I_0 Peak value incident intensity
L Slab thickness
R Hemispherical reflectance
s Geometric path length
t Time

Greek symbols

β Extinction coefficient
κ Absorption coefficient
μ Director cosine
Φ Scattering phase function
σ_s Scattering coefficient
θ Polar angle
ω Single scattering albedo
Ω Solid Angle

Subscripts

c Collimated
d Diffuse
i Incident

1. INTRODUCTION

Transient radiation transfer has found numerous applications in (1) laser-assisted micromachining, (2) remote sensing of combustion systems, and (3) of biological tissues among others [1]. The governing equation for radiation transfer in homogeneous, absorbing, non-emitting, and scattering media is the so-called radiative transfer equation (RTE). For one-dimensional transient radiation transfer along the *z*-direction on a gray basis it can be written as [2],

$$\frac{\partial I}{\beta c \partial t} + \frac{\mu}{\beta}\frac{\partial I}{\partial z} = -I + \frac{\omega}{4\pi}\int_{4\pi} I(\hat{\mathbf{s}}_i)\Phi(\hat{\mathbf{s}}_i, \hat{\mathbf{s}})\mathrm{d}\Omega_i \tag{1}$$

where ω is the single scattering albedo defined as $\sigma_s/(\kappa + \sigma_s)$ where the linear absorption and scattering coefficients are denoted by κ and σ_s, respectively. Here β is the extinction coefficient and c is the speed of light in the medium. The scattering phase function $\Phi(\hat{\mathbf{s}}_i, \hat{\mathbf{s}})$ represents the probability that radiation propagating in the solid angle $\mathrm{d}\Omega_i$ around direction $\hat{\mathbf{s}}_i$ will be scattered into the cone $\mathrm{d}\Omega$ around the direction $\hat{\mathbf{s}}$.

Established techniques for estimating the absorption and scattering coefficients as well as the scattering phase function consist of measuring the spectral or total, directional-hemispherical or directional-directional transmittance and reflectance, with collimated or diffuse incident radiation. First, initial values for the radiation characteristics are assumed and the RTE is solved. The calculated and measured quantities are compared and a new estimate of the radiation characteristics is made. This procedure is accomplished in an iterative manner until the set of absorption and scattering coefficients and scattering phase function minimizes the difference between the measured and the calculated properties. The major difficulty inherent to the inverse method is that there is no unique solution for the radiation characteristics. Moreover, due to the iterative nature of the method, the initial guess for radiation characteristics are of major importance if one wants a rapid convergence toward the optimum solution.

The present analysis aims at (1) gaining a physical understanding of transient radiation transfer in participating media, (2) performing a parametric study for the time-dependent hemispherical reflectance of a cold plane-parallel slab of an absorbing and isotropically scattering medium subject to a collimated Gaussian pulse, and (3) developing simple correlations for the maximum of the time-resolved hemispherical reflectance. The study pays particular attention to the maximum transient hemispherical reflectance which can easily be measured experimentally using a time-resolved attenuated total reflectance device [3]. Reflectance is preferred to transmittance as its magnitude and the associated signal to noise ratio are much larger, without requiring a powerful radiation source that could heat up or damage the samples. This issue is of particular concern for non-invasive in vivo sensing of biological tissues.

2. CURRENT STATE OF KNOWLEDGE

Due to the challenges encountered in solving the RTE several simplifying approaches have been suggested. First, the diffusion approximation has been used extensively in biomedical applications [3]. Its major advantage resides in the fact that there exist analytical solutions for the time-resolved hemispherical reflectance for simple geometries [3]. Brewster and Yamada [4] used the Monte Carlo method to study the effects of single scattering albedo, optical thickness, anisotropic scattering, and detector field of view on time-resolved transmittance and reflectance of an optically thick slab subjected to a picosecond collimated pulse. The numerical results were in good agreement with predictions of the diffusion approximation at long times [4]. The authors propose to use their findings to retrieve the radiation characteristics of absorbing and scattering media from transient transmission measurements at long times. However, their study also indicates that the diffusion theory predictions can be poor at early times, including the maximum hemispherical reflectance. Other studies have shown that the diffusion approximation fails to predict the transmittance at early times for all optical thicknesses and also at long times for optically thin slabs [5]. In addition, Guo *et al.* [6] showed that the diffusion approximation fails for both collimated radiation and strong anisotropically scattering media.

Moreover, analytical solutions of the transient RTE in homogeneous, isotropically scattering plane-parallel slab having a non-reflecting front surface with a blackbody back surface exposed to a collimated source have been obtained by Pomraning [7] and used by Wu [8] to obtain expressions for the hemispherical transmittance and reflectance. In addition, Wu [8] used the integral equation to compute the temporal reflectance and transmittance of 1-D absorbing and isotropically scattering slabs with various scattering albedos and optical thicknesses that compared well with results obtained using the Monte Carlo method. Tan and Hsu [9] used an integral formulation to simulate radiative transport in 1-D plane-parallel slab of a homogeneous absorbing and isotropically scattering medium with a black back surface exposed to diffuse or collimated irradiation. The authors then extended the method to solve the same problem in three-dimensional geometries [10].

Numerical techniques have also been used to solve the transient RTE. First, in a series of papers, Kumar and co-workers solved the transient radiation transfer equation for different geometries, scattering characteristics, and boundary conditions using various methods, including the P_1 approximation [11], Monte Carlo [12, 13, 14], discrete-ordinates (DOM) [5, 15, 16], and radiation element [17] methods and compared their results with predictions based on other methods or approximations [18] or with experimental data [16]. Moreover, Hsu [14] used the Monte Carlo method to study the effect of various parameters on the radiation transfer through a one-dimensional, plane-parallel, cold, absorbing, and isotropically scattering medium. The author focused on the transient local fluence within the slab by accounting for specular internal reflection at the slab surfaces. Also, Ayranci *et al.* [19] used the method of lines solution of the DOM to predict transmittance of a cubical enclosure of purely scattering media. Recently, Chai *et al.* [20] used the Finite Volume Method to simulate transient radiation transfer in a cube of absorbing and isotropically scattering medium with different boundary conditions and compared the results with published ones. On the other hand, Boulanger and Charette [21] used the DOM coupled with the piecewise parabolic advection (PPA) scheme to solve the transient multidimensional RTE for a collimated light pulse propagating in a semi-infinite, semi-transparent, non-homogeneous medium. Finally, Lu and Hsu [22] have developed the reverse Monte Carlo method in order to reduce the excessive computational time of the conventional Monte Carlo method and applied it to various geometries and scattering media. Similarly, Katika and Pilon [23] have developed the modified method of characteristics used in the present study. Advantages of this method versus other methods include its use for solving coupled equations using other numerical schemes, and its ability to capture the sharp discontinuities associated with the propagation of a radiation front in transient radiation transport.

Unfortunately, it was not possible to obtain analytical expressions [7, 8] for the maximum reflectance and the time at which it occurs. Instead, a numerical parametric study is performed using the modified method of characteristics and discussed in the following sections.

3. ANALYSIS

Let us consider transient radiation transfer in a homogeneous absorbing and isotropically scattering but non-emitting plane-parallel slab of thickness L. The front surface of the slab ($z = 0$) is exposed to a normally collimated and monochromatic incident Gaussian pulse. The index of refraction of the slab is assumed to be identical to that of the surroundings and equal to unity. Thus, the entire incident light is transmitted through the front surface and internal reflection can be ignored. The back surface of the slab ($z = L$) is treated as black and cold. This can be implemented by coating the surface with paints or soot particles depending on the wavelength of interest. Finally, a Gaussian pulse is considered instead of other pulse shapes as it closely matches the shape produced by lasers or light emitting diodes.

3.1. Governing Equation

To solve the one-dimensional RTE for collimated irradiation, the intensity is split into two parts: (i) the radiation scattered from the collimated radiation source and (ii) the remaining collimated beam after partial extinction by absorption and scattering along its path. The contribution from emission by the medium is negligible compared to the incident and scattered intensities, and consequently the medium can be considered as cold. Thus, the intensity for a gray medium is written as $I(z,\mu,t) = I_c(z,\mu,t) + I_d(z,\mu,t)$. The collimated intensity $I_c(z,\mu,t)$ at location z and time t in direction μ, remnant of any incident irradiation $I_i(t)$, is given by [2, 7], $I_c(z,\mu,t) = H(t-z/c)I_i(t-z/c)\delta(\mu-\mu_0)e^{-\beta z}$ where $\delta(\mu-\mu_0)$ is the Dirac's delta function, *H(t)* is the Heaviside step function and, in the present case, $\mu_0 = 1$. Thus the governing equation for the diffuse radiation intensity $I_d(z,\mu,t)$ along the characteristics curves of the photons [2, 24] can be written as,

$$\frac{1}{c}\frac{\mathrm{D}I_d(z,\mu,t)}{\mathrm{D}t} = -\beta I_d(z,\mu,t) + \frac{\sigma_s}{4\pi}\int_{4\pi} I_d(z,\mu_i,t)\mathrm{d}\Omega_i + \frac{\sigma_s}{4\pi}I_i(t-z/c)e^{-\beta z}H(t-z/c) \quad (2)$$

where DI_d/Dt is the total derivative of $I_d(z,\mu,t)$ along the characteristic curves $\mathrm{d}z/\mathrm{d}t = c\mu$.

3.2. Initial and Boundary Conditions

In order to solve the above governing equation, initial and boundary conditions must be specified. First, the initial intensity at all locations and in all directions at time *t* = 0 is taken as zero. At subsequent times, the radiation intensity incident on the front face (at *z* = 0) is a truncated Gaussian distribution with a pulse width t_p expressed as,

$$I_i(t) = I_0 \exp\left[-4\ln 2\left(\frac{t-t_c}{t_p}\right)^2\right], 0 < t < 2t_c \text{ and } I_i(t) = 0, t \geq 2t_c \quad (3)$$

In the present study, $I_i(t)$ reaches its maximum value I_0 at time $t_c = 3t_p$.

Finally, for the diffuse component, I_d, the front is transparent while the back surface is assumed to be black and cold, i.e., $I_d(z=0,\mu>0,t) = 0$ and $I_d(z=L,\mu<0,t) = 0$. The value of the diffuse intensity $I_d(z=0,\mu<0,t)$ and $I_d(z=L,\mu>0,t)$ need not be considered, because the method of solution uses boundary conditions only for intensity entering the computational domain [24].

3.3. Method of Solution

The governing Equation (2) and the associated boundary conditions are solved using the modified method of characteristics [24]. Extensive discussion of this method has been previously reported [23] and need not be repeated here. Comparison between numerical integral solutions [8] and the modified method of characteristics were found to be in good agreement with a mean error of less than 5% for $\beta L = 0.5$ and $\omega = 0.05$ and 0.95 [24]. The same accuracy is assumed in the present results. A uniform discretization of N_z points along the $z-$direction and N_θ discrete directions for θ varying from 0 to π was used. The time interval Δt had little effect on the numerical results as long as it satisfied $\Delta t \leq \Delta z/c$. Thus, Δt was set equal to $\Delta z/c$ where $\Delta z = L/(N_z-1)$. After solving for the time-dependent intensities in all the discrete directions at every point, the time-resolved hemispherical reflectance $R(t)$ at the front surface ($z=0$) can be computed based on the following definition, $R = -2\pi\int_{-1}^{0} I(0,\mu,t)\mu\mathrm{d}\mu$.

4. RESULTS AND DISCUSSION

A large range of optical thickness ($0 \leq \beta L \leq 50$), single scattering albedo ($0.05 \leq \omega \leq 1$), and incident pulse width ($0.015 \leq \beta ct_p \leq 0.15$) have been explored. The number of discrete points N_z and directions N_θ were varied between 100 and 2000 and between 50 and 450, respectively to obtain converged numerical solutions for each pair of parameters βL and ω. In all cases, the results were assumed to be numerically converged when doubling both N_z and N_θ produced less than 1% change in the value of the computed maximum hemispherical reflectance. The integrals were computed using the 3/8 Simpson's rule. The CPU time taken for computing the transient hemispherical reflectance for the case of $\beta L = 0.5$ and $\omega = 0.95$, for example, using a spatial discretization of $N_z = 101$ points and an angular discretization of $N_\theta = 25$ directions per octant was about 21 seconds on a 512 MHz Pentium III for a total dimensionless time of t^* (= βct) = 8.

4.1. Effect of βL and ω

Figure 1 shows the typical transient hemispherical reflectance of the plane-parallel slab with a black back surface as a function of βct, for $\omega = 0.7$, $\beta L = 0.7$, and $\beta ct_p = 0.15$. Since there is no direct reflection of the incident beam from the front surface, the reflected signal is due to back scattering of the incident radiation by the slab. The maximum value of the reflectance is denoted by R_1 and occurs at dimensionless time βct_1. For a black back surface, the reflectance reveals only one maximum as the pulse is absorbed once it reaches the back of the slab.

Moreover, *Figure 1* shows the transient hemispherical reflectance as a function of the dimensionless time t^* for different values of the single scattering albedo ω and for βL = 0.7 and $\beta ct_p = 0.15$. Similar plots have been obtained for other values of βL. One can see that the hemispherical reflectance R increases as ω increases for any given dimensionless time βct. This can be attributed to the increase in the scattering coefficient resulting in a larger fraction of the incident intensity being back-scattered by the medium.

Finally, *Figure 1* plots the transient hemispherical reflectance as a function of the dimensionless time βct for different values of βL and for ω = 0.95 and $\beta ct_p = 0.15$. Similar results have

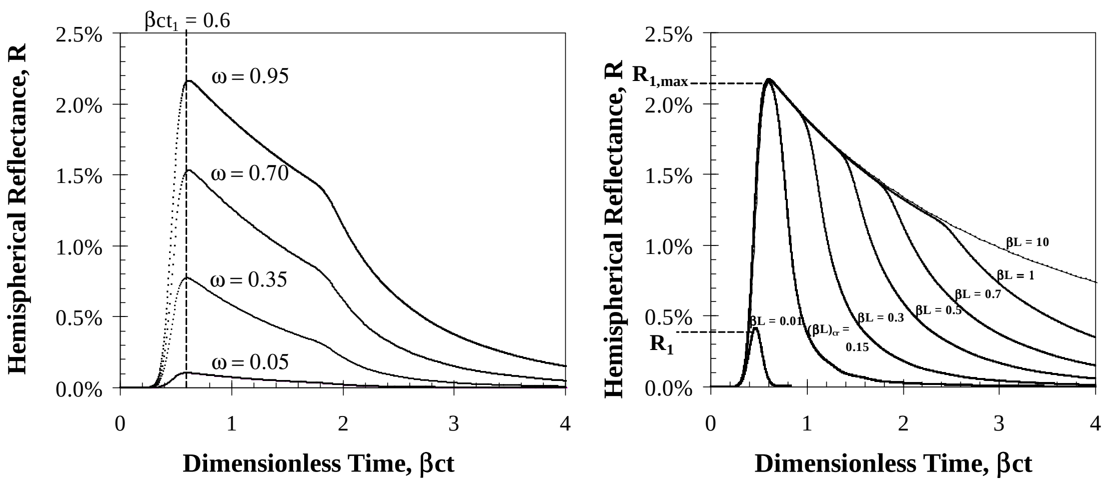

Fig. 1 - Hemispherical reflectance as a function of βct for different values of ω for $\beta L = 0.7$ (left) and for different values of βL (right) $\omega = 0.95$. In both graphs $\beta ct_p = 0.15$.

been obtained for different values of ω. *Figure 1* indicates that as the maximum reflectance R_1 increases with βL up to a critical optical thickness $(\beta L)_{cr}$ beyond which it is independent of βL. The highest value for the maximum reflectance is denoted $R_{1,max}$. One can also note that $(\beta L)_{cr}$ for this case is equal to 0.15 which, coincidentally, is also the value of βct_p. The effect of the incident pulse width, βct_p, will be discussed in detail in section 4.3.

4.2. Maximum Reflectance

Let us now focus our attention to the value of the maximum reflectance R_1 as a function of the optical thickness βL and of the single scattering albedo ω. *Figure 2* shows the peak value of the transient reflectance R_1 as a function of the optical thickness βL ranging from 0.01 to 50 for (left) $\beta ct_p = 0.15$ and for (right) five different values of the single scattering albedo between 0.05 and 1. Moreover, optically thin and optically thick regimes can be identified as follows:
Optically Thin Regime, $\boldsymbol{\beta L \leq (\beta L)_{cr}}$. In this regime, R_1 varies linearly with ln(βL) and increases as ω increases and $(\beta L)_{cr}$ depends on the pulse width βct_p.
Optically Thick Regime, $\boldsymbol{\beta L > (\beta L)_{cr}}$. In this regime, R_1 is independent of βL but increases with ω. Beyond the critical value $(\beta L)_{cr}$, the optical thickness βL has no effect on the maximum reflectance, and R_1 reaches its maximum denoted by $R_{1,max}$.

4.3. Effect of the Incident Pulse Width

To investigate the effect of the dimensionless pulse width on the hemispherical reflectance, different values of βct_p have been investigated, namely 0.15, 0.075, and 0.015. *Figure 2* (left) plots the maximum hemispherical reflectance R_1 versus βL for different values of βct_p at $\omega = 0.7$. One can see that R_1 increases as βct_p increases for fixed values of ω and βL. This can be

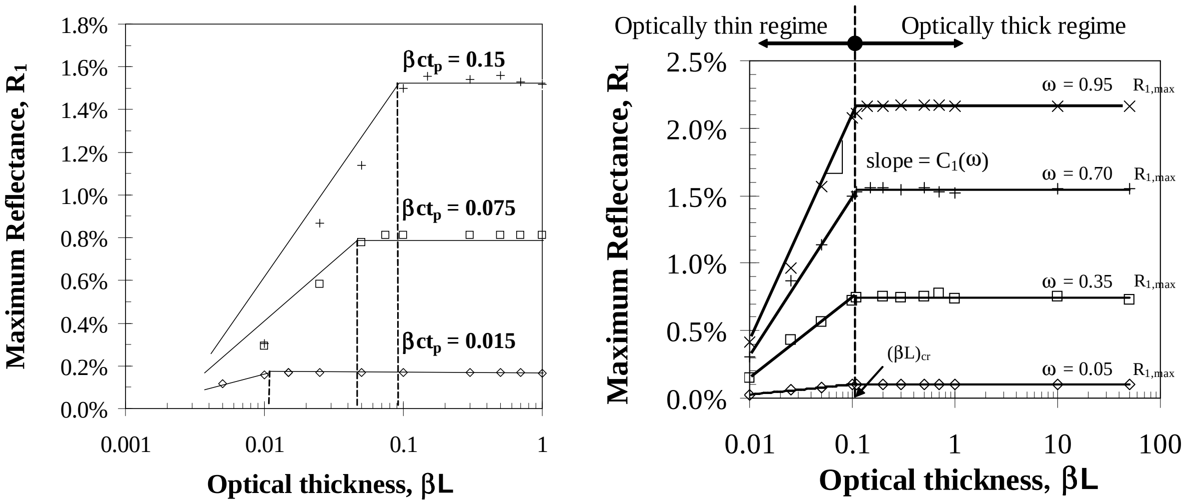

Fig. 2 - Effect of the dimensionless pulse width βct_p for $\omega = 0.7$ (left) and the effect of the single scattering albedo ω and of the optical thickness βL for $\beta ct_p = 0.15$ (right) on R_1.

attributed to the fact that increasing the pulse width increases the radiant energy in the slab at any given time and therefore, increases the scattered radiation intensity and the reflectance.

In addition, *Figure 2* (right) and *Figure 3* show R_1 as a function of βL for different values of the single scattering albedo ω. It indicates that βL reaches βct_p the value of R_1 becomes independent of βL. This is defined as the optically thick regime because increasing βL no longer has any effect on the value of R_1. In the optically thick regime $R_1 = R_{1,max}$.

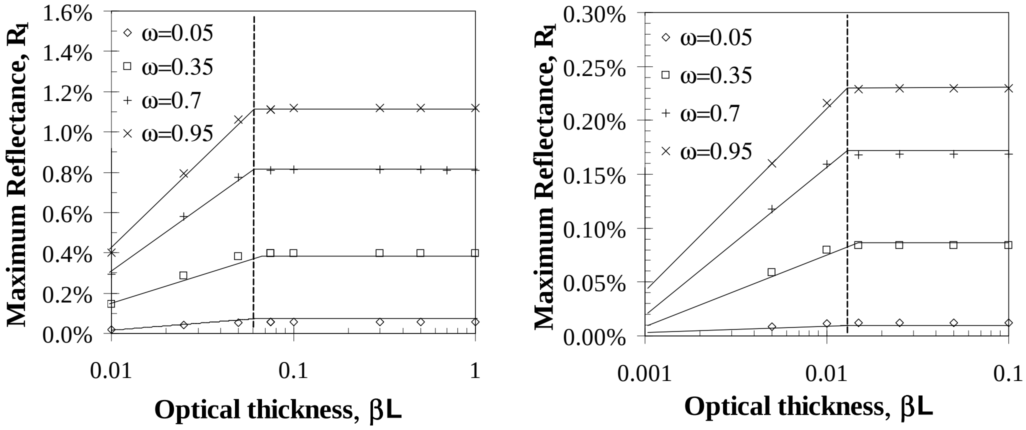

Fig. 3 - R_1 as a function of βL and ω for $\beta ct_p = 0.075$ (left) and 0.015 (right).

Finally, for each value of ω, the values of $(\beta L)_{cr}$ can be obtained from R_1 versus βL. The values of $(\beta L)_{cr}$ vary within 5%. *Figure 4* shows the average critical optical thickness $(\beta L)_{cr}$ as a function of the dimensionless pulse width βct_p for different values of ω. One can see that for $\beta ct_p = 0.015$ and 0.075, the average value of the critical optical thickness $(\beta L)_{cr}$ is approximately βct_p. However, when βct_p increases to 0.15, the average value of $(\beta L)_{cr}$ falls below βct_p possibly due to numerical error. Nonetheless, this finding indicates that $(\beta L)_{cr}$ is equal to βct_p within 10%.

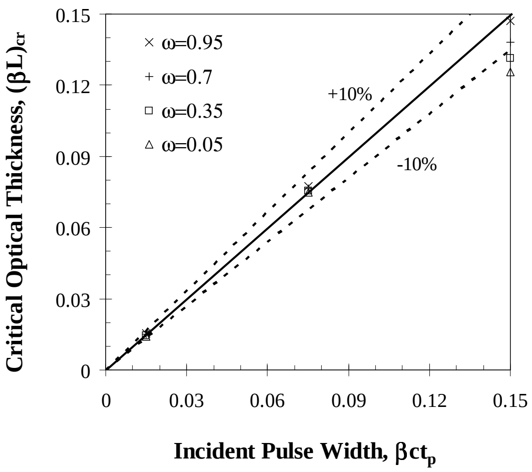

Fig. 4 - Effect of the dimensionless pulse width βct_p and ω on the critical βL.

4.4. Correlations

Developing correlations for transient hemispherical reflectance could be useful as a simple method for retrieving the optical thickness and the single scattering albedo of a substance. Then,

each regime features its own set of correlations for R_1.
Optically Thin Regime, $\beta L \leq \beta ct_p$. In this regime the maximum reflectance R_1 varies linearly as a function of ln(βL) as indicated by Figure 2 and can be expressed as,

$$R_1(\omega, \beta ct_p, \beta L) = C_1 \ln(\beta L) + C_2 \tag{4}$$

where the slope $C_1(\omega, \beta ct_p)$ and the constant $C_2(\omega, \beta ct_p)$ depend on both ω and βct_p. *Figure 5* illustrates the values $C_1/\beta ct_p$ and $C_2/\omega\beta ct_p$ as functions of ω and βct_p, respectively for $\beta L \leq \beta ct_p$. It shows that both C_1 and C_2 vary with $\omega\beta ct_p$ according to,

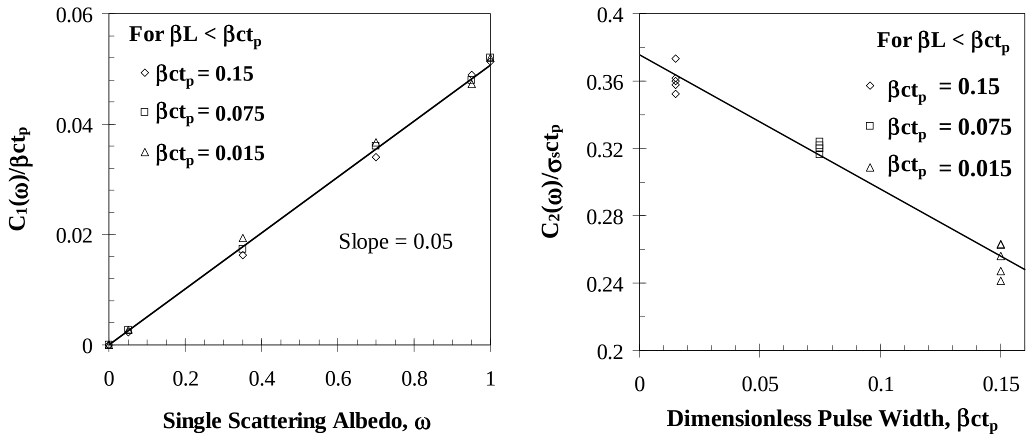

Fig. 5 - Value of the slope $C_1/\beta ct_p$ (left) and constant $C_2/\sigma_s ct_p$ (right) as a function of the single scattering albedo, ω, and the incident pulse width, βct_p, respectively for $\beta L < \beta ct_p$.

$$C_1 = 0.05\omega\beta ct_p = 0.05\sigma_s ct_p \quad \text{and} \quad C_2 = (-0.8\beta ct_p + 0.375)\sigma_s ct_p \tag{5}$$

This confirms that if the slab is non-scattering $(\sigma_s = 0)$ its reflectance vanishes. The squared coefficients of correlation, R^2, for C_1 and C_2 are 0.998 and 0.973, respectively.
Optically Thick Regime, $\beta L > \beta ct_p$. In this regime, the maximum reflectance $R_{1,max}$ is independent of βL. *Figure 6* shows the linear increase of the ratio $R_{1,max}/\beta ct_p$ as a function of ω. It establishes that $R_{1,max} = 0.156\sigma_s ct_p$ for $\beta L > \beta ct_p$.

4.5. Discussion

First, numerical simulations were performed for different indices of refraction (*n* = 1, 1.33, and 1.5) for $\omega = 0.7$ and $\beta L = 0.5$ while still neglecting internal reflectance. This can be achieved practically by immersing the device in an index matching fluid whose index of refraction is the same as that of the slab to be analyzed. As expected from dimensional analysis, the same values of the transient hemispherical reflectance shown were obtained for the same set of parameters ($\omega, \beta L, \beta ct_p$).

Moreover, a comparison between the prediction of the above correlations with numerically computed values of R_1 was performed. The computed maximum hemispherical reflectance is properly predicted within a maximum absolute error of $\pm 0.21\%$. The maximum relative error was determined for small values of R_1 which, in any event, might be difficult to measure experimentally.

Finally, the above correlations could be used to determine the radiation characteristics of homogeneous absorbing and isotropically scattering media by experimentally measuring the

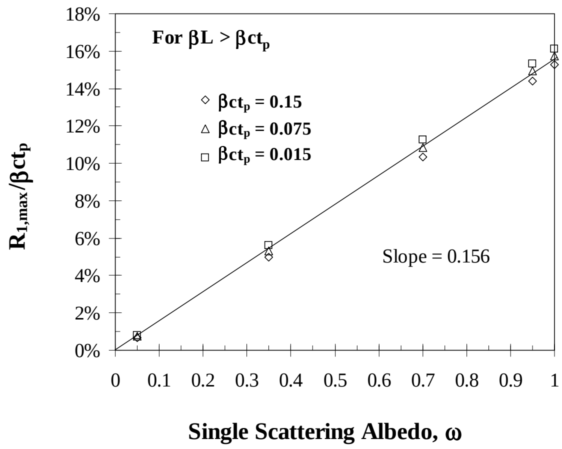

Fig. 6 - Maximum hemispherical reflectance scaled with $\beta c t_p$, as a function of the single scattering albedo ω in the optically thick regime ($\beta L > \beta c t_p$).

maximum of the transient reflectance for slabs having at least two different thicknesses or by holding $t_c = 3t_p$ and varying the pulse width of the incident radiation. The slab thickness or the pulse width are chosen to cover both the optically thin and thick regimes. Note that this bears some analogy with the method proposed by Yamada and Kurosaki [25] to retrieve the radiation characteristics of porous materials from *steady-state* emittance measurements. Indeed, the authors assumed an isotropic scattering phase function and used the fact that the emittance of an optically thick and isotropically scattering medium is independent of the optical thickness and depends only on the single scattering albedo. Thus, the method could also serve to obtain an initial guess for more complex inversion schemes accounting for anisotropic scattering.

5. CONCLUSIONS

This paper proposes a method to determine the radiation characteristics of homogeneous, cold, absorbing and isotropically scattering plane-parallel slab with a transparent front surface and a black back surface from measured time-resolved hemispherical reflectance. It presents a parametric study focusing on the maximum hemispherical reflectance R_1. Dimensionless parameters include the optical thickness of the slab βL, the single scattering albedo ω, and the incident pulse width $\beta c t_p$. Conclusions of the study are as follows: **(1)** there exist optically thin and optically thick regimes for the maximum hemispherical reflectance R_1, **(2)** these two regimes meet at a critical optical thickness $(\beta L)_{cr}$ such that $(\beta L)_{cr} \approx \beta c t_p$, **(3)** in the optically thin regime, R_1 increases with increasing βL, ω and $\beta c t_p$, **(4)** in the optically thick regime, $R_{1,max}$ is proportional to $\omega \beta c t_p$ and is independent of βL.

Similar parametric studies could be performed for (i) other pulse shapes, (ii) independently varying t_c and t_p of the Gaussian pulse, (iii) cases when the indices of refraction across the front surface differ and one needs to account for internal reflection, and (iv) anisotropically scattering media. Similar trends and correlations are anticipated.

REFERENCES

[1] KUMAR, S. and MITRA, K., "Microscale aspects of thermal radiation transport and laser applications", *Advances in Heat Transfer*, vol. 33, pp. 187–294, 1999.

[2] MODEST, M.F., *Radiative Heat Transfer*, Academic Press, San Diego, CA, 2003.

[3] PATTERSON, M.S., CHANCE, B. and WILSON, B.C., "Time resolved reflectance and transmittance for the non-invasive measurement of tissue optical properties", *Applied Optics*, vol. 28, no. 12, pp. 2331–2336, 1989.

[4] BREWSTER, M.Q. and YAMADA, Y., "Optical properties of thick, turbid media from picosecond time-resolved light scattering measurements", *Int. JHMT*, vol. 38, pp. 2569–2581, 1995.

[5] ELALOUFI, R., CARMINATI, R. and GREFFET, J.J., "Time-dependent transport through scattering media: from radiative transfer to diffusion", *J. of Optics A: Pure And Applied Optics*, vol. 4, no. 5, pp. S103–S108, 2002.

[6] GUO, Z. and KIM, K., "Ultrafast-laser-radiation transfer in heterogeneous tissues with the discrete-ordinates method", *Applied Optics*, vol. 42, pp. 2897–2905, 2003.

[7] POMRANING, G.C., *The Equations of Radiation Hydrodynamics*, Pergamon Press, New York, 1973.

[8] WU, C-Y., "Propagation of scattered radiation in a participating planar medium with pulse irradiation", *JQSRT*, vol. 64, no. 5, pp. 537–548, 2000.

[9] TAN, Z.-M. and HSU, P.-F., "An integral formulation of transient radiative transfer", *ASME J. of Heat Transfer*, vol. 123, pp. 466–475, 2001.

[10] TAN, Z.-M. and HSU, P.-F., "Transient radiative transfer in three-dimensional homogeneous and non-homogeneous participating media", *JQSRT*, vol. 73, pp. 181–194, 2002.

[11] MITRA, K., LAI, M.S. and KUMAR, S., "Transient radiation transport in participating media within a rectangular enclosure", *J. of Thermophysics and Heat Transfer*, vol. 11, pp. 409–414, 1997.

[12] GUO, Z., KUMAR, S. and SAN, K.-C., "Multidimensional Monte Carlo simulation of short-pulse transport in scattering media", *J. of Thermophysics and Heat Transfer*, vol. 14, pp. 504–511, 2000.

[13] GUO, Z. and KUMAR, S., "Three-dimensional discrete ordinates method in transient radiative transfer", *J. of Thermophysics and Heat Transfer*, vol. 16, no. 3, pp. 289–296, 2002.

[14] HSU, P.-F., "Effects of multiple scattering and reflective boundary", *Int. J. of Thermal Sciences*, vol. 40, pp. 539–549, 2001.

[15] GUO, Z. and KUMAR, S., "Discrete-ordinates solution of short-pulsed laser transport in two-dimensional turbid media", *Applied Optics*, vol. 40, pp. 3156–3163, 2001.

[16] GUO, Z. and KUMAR, S., "Three-dimensional discrete ordinates method in transient radiative transfer", *J. of Thermophysics and Heat Transfer*, vol. 16, pp. 289–296, 2002.

[17] GUO, Z. and KUMAR, S., "Radiation element method for transient hyperbolic radiative transfer in plane-parallel inhomogeneous media", *Numerical HT: Part B*, vol. 39, pp. 371–387, 2001.

[18] MITRA, K. and KUMAR, S., "Development and comparison of models for light pulse transport through scattering-absorbing media", *Applied Optics*, vol. 38, pp. 188–196, 1999.

[19] AYRANCE, I. and SELÇUK, N., "MOL solution of DOM for transient radiative transfer in 3-D scattering media", *JQSRT*, vol. 84, pp. 409–422, 2004.

[20] CHAI, J.C., HSU, P.-F. and LAM, Y.C., "Three-dimensional transient radiative transfer modeling using the finite-volume method", *JQSRT*, vol. 86, pp. 299–313, 2004.

[21] BOULANGER, J. and CHARETTE, A., "Reconstruction optical spectroscopy using transient radiative transfer equation and pulsed laser: a numerical study", *JQSRT*, vol. 93, pp. 325–336, 2005.

[22] LU, X. and HSU, P.-F., "Reverse Monte Carlo simulations of light pulse propagation within three-dimensional media", *J. of Thermophysics and Heat Transfer*, vol. 19, no. 3, pp. 353–359, 2005.

[23] PILON, L. and KATIKA, K., "Backward method of characteristics for simulating microscale energy transport", *ASME J. of Heat Transfer*, vol. 126, pp. 735–743, 2004.

[24] KATIKA, K. and PILON, L., "Modified method of characteristics for transient radiative transfer", *JQSRT*, vol. 98, pp. 220–237, 2006.

[25] YAMADA, J. and KUROSAKI, Y., "Estimation of a radiative property of scattering and absorbing media", *Int. J. of Thermophysics*, vol. 18, no. 2, pp. 547–556, 1997.